X-ray diffraction study of deformation state in InGaN/GaN multilayered structures

V.P. Kladko, A.V. Kuchuk, N.V. Safryuk, V.F. Machulin, A.E. Belyaev, R.V. Konakova, B.S. Yavich[1]
V. Lashkaryov Institute of Semiconductor Physics, NAS of Ukraine,
41, prospect Nauky, 03028 Kyiv, Ukraine
[1]CJSC "Svetlana-Optoelectronics", St.-Petersburg, POB 78, 194156 Russia

Abstract. High resolution X-ray diffractometry (HRXRD) was used to investigate $In_xGa_{1-x}N$/GaN multilayered structures grown by the metal-organic chemical vapor deposition (MOCVD) method. Deformation conditions in the superlattice (SL) and its separate layers, degree of relaxation in the structure layers, as well as the period of the SL, thicknesses of its layers and composition of In_xGa_{1-x} solid solution in active area were determined. It was found that SL was grown on the relaxed buffer layer. SL layers were grown practically coherent with slight relaxation of InGaN layer (about 1.5 %). The role of dislocations in relaxation processes was established. Analysis of experimental diffraction spectra in these multilayered structures within the frameworks of Parrat-Speriozu was adapted for hexagonal syngony structures.

Keywords: high resolution X-ray diffractometry, multilayered structure, deformation characteristics.

1. Introduction

Multilayered epitaxial structures (nanoheterostructures) based on InGaN/GaN solid solutions are widely used to fabricate light-emitting diodes (LED) for visible and UV bands [1-3].

For these structures, large mismatches of lattice parameters are typical, which are caused by strain fields that results in appearance of strong piezoelectric fields [4, 5]. In addition, a large density of dislocations, interface roughness, composition fluctuations are inherent to these structures. Such a situation results in deterioration of optical properties of these structures. Therefore, the rise of efficiency and broadening the spectral band for LED is one of the main trends in current technology of nanoheterostructures.

Consequently, the investigation of the defects nature and deformation state of these systems is an urgent problem for both production process providing layers with different electron potential and understanding the influence of these effects on electronic devices performance. Growing the various intermediate buffer layers makes it possible to compensate mismatch stresses and improve crystalline perfection of heterostructures.

X-ray diffractometry is used to determine structural (geometrical) parameters of multilayered systems, such as composition and thickness of separate layers, as well as sequence of their arrangement [6-10]. Besides, the rocking curves contain information concerning the sharpness of heteroboundaries (the presence of transitional layers), the strain inside layers as well as structural perfection of epitaxial layers and composition, the type of defects and their parameters.

Some aspects of the X-ray diffractometry implication for the investigation of InGaN/GaN multilayered epitaxial structures and for determination of structural and deformational parameters are considered in this work.

2. Samples and experimental technique

X-ray study was carried for samples based on InGaN/GaN grown by metal organic chemical vapor deposition method of hybrid epitaxy (MOCVD) on (0001) sapphire substrates. The quantum wells (QW) composition was uniform and adjusted to emit the wavelength close to 460 nm. Nominal composition of InGaN was within the range of 12-15 % In content. The samples consist of low temperature nucleation GaN-layer grown on the sapphire substrate, 3.5-μm thick *n*-GaN buffer layer, buffer five-periods SL (the thicknesses of QW was 2.5 nm and GaN barrier − 4-5 nm), and active region which contains five InGaN/GaN QWs, 20-nm thick current locking *p*-AlGaN layer, and 0.1-μm thick *p*-GaN-layer. The nominal thicknesses of QW and quantum barrier were 2.5 and 9 nm, respectively.

The measurements were performed using "PANalytical X'Pert PRO MRD" high resolution diffractometer for symmetric (000*l*) and asymmetric (–1–124) reflections. The experimental setup makes it possible to obtain two cross-sections of the reciprocal lattice nodes – transversal to the diffraction vector, ω-scan, and in parallel to it, ω–2θ-scan. Triple-axis diffractometry provides a mean for separation of the effects of interplane spacing changes and atomic plane rotation, therefore, analysis of the intensity distribution in q_x, q_y coordinate system, directed along and normal to **H**-vector, respectively, makes it possible to separate each of these contributions separately [8, 9]. The macrodeformations that cause the sample bending were estimated by the system curvature radius determined by the measurement of the changes in the reflection angles from sapphire reflection during linear scanning of the sample along X-ray beam [11].

The following structural parameters were used in this work. GaN: $a = 3.1896\pm0.0003$ Å, $c = 5.1855\pm0.0002$ Å, $c/a = 1.6258\pm0.0002$; $p = 0.53$ [12]; InN: $a = 3.5378\pm0.0001$ Å, $c = 5.7033\pm0.0001$ Å, $c/a = 1.6121\pm0.0001$; $p = 0.49$ [13].

3. The model of X-ray diffraction for multilayered structures (MS)

Superlattice (SL) represents periodical sequence of two alternating layers with different composition. Coherent two-layered superlattice with sharp heteroboundaries is characterized by four main parameters: the period T, the thickness ratio of two layers t_1/t_2, the compositions of the layers x_1 and x_2, which determines the interplane spacing in the layers d_1 and d_2 and their structural factors F_1 and F_2. The number of parameters is reduced to two, if SL consists of pure element layers (for example AlN/GaN). Three parameters are used in the case when one of the layers is a ternary solid solution (*e.g.*, In$_x$Ga$_{1-x}$N/GaN). Typical rocking curve from SL has two systems of oscillations – periodical intensity distributions depending on the incident angle (see Fig. 1). The first system represents the thickness oscillations which are typical for any reflection from thin layer, and the second one represents periodically distributed satellites, caused by periodical distribution of the interplane spacing $d(z)$ and dispersion capacity $F(z)$ throughout the crystal depth.

In most cases, rocking curves elude analyzing because of blurring of heteroboundary, close compositions of layers, *etc*. Thus, obtaining the real structural parameters from the rocking curves requires the fitting calculation of diffraction reflections.

The reflection coefficient of MS in the semi-kinematical approximation [14] is given by:

$$R = \left| A_0 + iA_L \right|^2, \tag{1}$$

where A_0 is the amplitude of dynamic reflection from the substrate:

$$A_0 = \left| |y| - \sqrt{y^2 - 1} \right|, \tag{2}$$

and A_L is the kinematical amplitude of a surface structure calculated as a sum of reflection amplitudes for individual layers:

$$A_L = \sum_{i=1}^{n} \frac{\sin[(y - f_i)u_i] K_i}{y - f_i} \exp(-i\varphi_i). \tag{3}$$

The phase φ_i takes into account individual phases of each *i*-layer as well as phase progression inside lower layers and can be calculated as:

$$\varphi_i = (y - f_i)u_i + \sum_{k=1}^{i-1} 2(y - f_k)u_k. \tag{4}$$

$u = \pi \cdot t / \Lambda$ is the reduced thickness, Λ – length of extinction.

In the general case of asymmetric diffraction for coherent systems, reduced angle displacement is equal to

$$y = \frac{\Delta\theta \sin(2\theta)}{|\chi_H|} \sqrt{\frac{\gamma_0}{|\gamma_H|}}, \tag{5}$$

where $\Delta\theta$ angle is reckoned from the substrate peak. Reduced deformation

$$f_j = -\varepsilon_{zz}^j \frac{(\gamma_H - \gamma_0)\gamma_H}{|\chi_H|} \sqrt{\frac{\gamma_0}{|\gamma_H|}} \tag{6}$$

is the reflection centre of *i*-th layer in the *y*-scale, and the thickness of layers u is expressed in fractions of the extinction length. The quantities $K_i = |F_i| / |F_0|$ take into account the difference of structural factors F_i of the layer and F_0 of the substrate.

For superlattices, summation (3) is carried out only for two layers that make the period. Let us determine an appropriate value as a structural factor for SL F_{SL}, but the total scattering amplitude is equal to:

$$A_{SL} = F_{SL} \frac{\sin(m\Phi)}{\sin(\Phi)} \exp[-i(m-1)\Phi], \tag{7}$$

where

$$\Phi = (y - f_1)u_1 + (y - f_2)u_2. \tag{8}$$

If the denominator in (7) is equal to zero ($\Phi = n\pi$), we obtain the angle position of *n*-th satellite, if the numerator is equal to zero, we obtain the position of thickness oscillation.

As is seen from (7), the satellites intensity is determined by F_{SL} values in these angular positions. According to [15], the intensity of zero satellite with the angle position y_0 is equal to:

$$J_0 = \left[\frac{\sin((y - f_2)u_2)}{(y - f_2)u_2} \right]^2 (u_1 + u_2)^2 m^2. \tag{9}$$

Quantity $(y_0 - f_2)u_2 = -(y_0 - f_1)u_1$ (let us denote it as *B*) can be expressed as:

$$B \equiv \pi S \Delta\varepsilon \frac{t_1 t_2}{t_1 + t_2} \cos\varphi, \qquad (10)$$

where $\Delta\varepsilon$ is the relative difference of interplane spacings (normal to the surface) of two layers $\Delta\varepsilon = 2(d_2 - d_1)/(d_2 + d_1)$. The first factor in equation (4) shows dependence of B on the order of reflection. Intensities of other satellites can be analytically expressed as a function of SL parameters. This function is proportional to the total thickness of SL. But the relative intensity of satellites with respect to the zero-satellite height will be independent of the number of superlattice periods and can be written as:

$$\frac{J_n}{J_0} = \left[\frac{\sin(B+na)}{B+na} \left(a - \frac{K \cdot (B+na)(\pi-a)}{-B+n(\pi-a)} \right) \right]^2 \Bigg/ \left(\frac{\sin B}{B} \right)^2, \qquad (11)$$

where $a = \pi/(1 + t_2/t_1)$. The relative intensity of satellites is the function of three unknown quantities: the parameter of deformation B, the ratio of thicknesses of two layers $b = t_2/t_1$, and ratio of their structural factors $K = F_2/F_1$. Period T is involved implicitly through B value. Using the expressions (10) and (11) makes it possible to replace the intensity fitting of the whole rocking curve from SL by calculation of intensity for particular angular points, namely, the satellites maxima.

In the majority of cases, the parameter B exerts the biggest influence on the shape of rocking curve from SL. Its value can be increased due to the rise of both lattice mismatch of two layers and SL period growth. Certainly, absolute intensity values and their angle range will be different. The higher B value, the higher is the intensity of side satellites in comparison with zero satellite, all other factors being equal, and for $B > \pi/2$ zero satellite can become lower than side satellites. In this case, a problem with identification of zero satellite arises.

In another limiting case, for small values of B, the intensity of side satellites decays fast, and at $B < 0.1$ only the first order satellites can be observed. Reduction of B is achieved not only by $\Delta\varepsilon$ and T reduction, but also by reduction of one of the layer thickness at a constant period. For the SL parameter-matched solid solutions ($B = 0$), side satellites appear at the expense of structural factors difference. The relative intensity of these satellites is expressed by a simple formula:

$$\frac{J_n}{J_0} = \left(\frac{\sin(n\pi t_2/T)}{n\pi t_2/T} \right)^2 \left| \frac{t_2(1-K)}{t_1 + t_2 K} \right|^2. \qquad (12)$$

As the expression (12) suggests, the curve must be symmetric, and the intensity of side satellites reduces rather slowly, if one layer is much thinner than another one.

There are two parameters of the superlattice that can be determined directly from rocking curves. The period T can be obtained from satellites spacing $\delta\theta$, and average interplane spacing $\langle d \rangle$ can be obtained from the angle between the central superlattice (zero-satellite) peak and substrate peak. We can calculate unknown values of B,

b, and k from relative satellites intensities (if their number on the experimental curve exceeds three, including zero-satellite). We need only these quantities to calculate all four parameters of coherent SL. However, it takes place for an ideal case only. The sensitivity of satellites intensity to b and K values depends on their change intervals. It can be very low that prevents to determine peaks with a sufficient accuracy.

For the case when one of the layers is much thinner than another ($b << 1$), which takes place in multilayered quantum wells, the parameter B depends on product of mismatch and thin layer thickness only, and represents phase shift of waves, diffracted by thick layer and caused by the presence of thin layer.

$$B \approx \Delta\varepsilon t_2. \qquad (13)$$

This product also determines an average interplanar spacing in superlattice and angular position of zero-satellite. Thus, the number of parameters that can be obtained from a diffraction curve reduces to three.

Real structures will differ from the two-layered system with sharp heteroboundaries. Possible blurring of interfaces and the presence of additional buffer and coating layers in the heterosystem effect on the shape of diffraction rocking curve. However, in all cases the two-layered structure can be considered as the first approximation, which can be used to obtain initial parameters for their further improvement by simulation of curves and fitting procedure.

4. Results and discussions

The experimental double-crystal (1) and triple-axis (2) diffraction rocking curves and calculated spectrum (3) of symmetric reflection 0002 are presented in Fig. 1.

These rocking curves contain two systems of satellites: system from main SL and that from buffer SL with lower intensity and fewer satellites. Position of zero satellite on this picture is blurred by buffer GaN peak having a strong diffuse component.

Diffraction rocking curves from SL contain two systems of oscillations – periodic intensity distribution depending on the incidence angle – "fast" oscillations, which are typical for reflection from the thin layer or the whole structure, and periodically located satellites (S_n) up to the second order, which testify good periodicity of grown structures. The splitting of zero satellite observed in the experimental rocking curve cannot be explained by oscillations of the thickness. As we can see from simulation results, this is the influence of the cover layer, which provides reflection in the zero satellite region of main SL. We cannot estimate indium content inside QW of buffer SL from experimental spectra, because it is under the influence of zero satellite region of the active SL, coating layer and GaN buffer layer. This issue can be solved by simulation of the structure spectra. This simulation provides indium content of about 8-10 %.
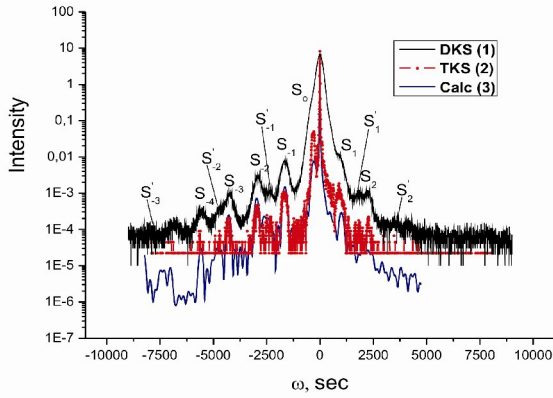
Fig. 1. ω–2θ-scans for symmetric reflection 0002 for $In_xGa_{1-x}N/GaN$ SL grown on buffer layer GaN and calculated data. S_n – satellites of active SL, S'_n – satellites of buffer SL.

The period T and the average interplanar spacing $\langle d \rangle$ are obtained immediately from rocking curves of SL: T – from the spacing between two satellites $\delta\theta$:

$$T = \frac{|\gamma_h|\lambda}{\sin(2\theta_B)\,\delta\theta}, \qquad (14)$$

$\langle d \rangle$ – from the angle between the substrate peak and central peak from SL (zero satellite):

$$(\Delta d/d)_\perp = \frac{\langle d \rangle - d_0}{d_0} = -\Delta\theta / \left(\mathrm{tg}(\theta_B) \cdot \frac{2|\gamma_h|}{\gamma_0 + |\gamma_h|} \right). \quad (15)$$

For epitaxial structures of hexagonal syngony grown in plane (0001)

$$(\Delta d/d)_\perp = \Delta c/c + p(\Delta a/a), \qquad (16)$$

where $p = 2c_{13}/c_{33}$ (c and a are parameters of the hexagonal unit cell).

Knowing these values will suffice to determine parameters of superlattices consisting of pure substances.

Let us note that there is no substrate peak on rocking curves obtained from nitride films grown on sapphire (the nearest reflection from sapphire is located out of the measured angular interval). This substrate peak usually serves as a datum point for determination of buffer epitaxial layers deformation. Therefore, an absolute scale of reflection angles should be used to obtain a and c parameters. An analyzer was used to measure the scattering angle 2θ for GaN layer and central SL peak.

For defect structures similar to the system under investigation, the satellites are broadened due to the influence of defects [16]. However, in actual practice all satellites of SL are distorted in the same manner (if only influence of defects, and not the mistakes in the SL sequence are taken into account), that makes it possible to compare the calculated curve (for ideal SL) and experimental (distorted) rocking curves by relative height of satellites or their integral intensity.

However, to obtain full information about structure parameters one should calculate the reflectivity spectra.

The parameters of SL obtained using this method and adjusted using the fitting procedure for experimental and calculated curves are presented in Table.

The expression (15) holds if epitaxial layers have coherent borders, *i.e.*, the system is not relaxed. The relaxation of elastic stresses (basically, mismatch and thermal stresses) can proceed by different mechanisms [17, 18]. The main one is appearance of mismatch dislocations grid. In this case, the tangential mismatch $(\Delta d/d)_\parallel$ appears in the vicinity of normal mismatch $(\Delta d/d)_\perp$. (For unrelaxed systems, the distances between planes perpendicular to heterointerface are identical for all the layers and the substrate). On the rocking curves, the relaxation manifests itself in angular shift and broadening the diffraction peaks in comparison with those in elastically deformed system. However, from the angular position of peaks for symmetric Bragg reflections we cannot draw the conclusion that a certain layer is elastically deformed or relaxed, if the composition of this layer is unknown. From measurements of asymmetric reflections, values of the average parameter of superlattices a were determined $\langle a \rangle = (a_1 t_1 + a_2 t_2)/T$.

Then real parameters c_i and a_i were determined from the values B, $\langle c \rangle$ and $\langle a \rangle$ for both layers of SL. From these parameters, the In content in InGaN layer and distribution of changes in the c parameter over the SL thickness were established. All these data are presented in Table and Fig. 2.

Table.

Layers of the structure	t, nm	c, nm	a, nm	$\varepsilon_\perp$	x	c/a
InGaN-SL1	3.5	0.52987	0.32309	0.01410	0.18	1.6400
GaN-SL1	9.0	0.51744	0.31871	−0.00561	−	1.6235
InGaN-SL2	3.5	0.53007	0.32313	0.01560	0.07	1.6404
GaN-SL2	3.8	0.51713	0.31887	−0.00645	−	1.6217

The triple-axis geometry of diffraction makes it possible to determine epitaxial structures using the analysis of the so-called maps of the intensity distribution around reciprocal space nodes (RSM) [19]. It is based on the fact that the intensity of coherent scattering from completely stressed epitaxial heterostructures is distributed in the scattering plane in direction parallel to the surface normal. In this direction, additional nodes, such as the centers of reflection from separate layers, the thickness oscillations, and satellites of superlattice, are located.
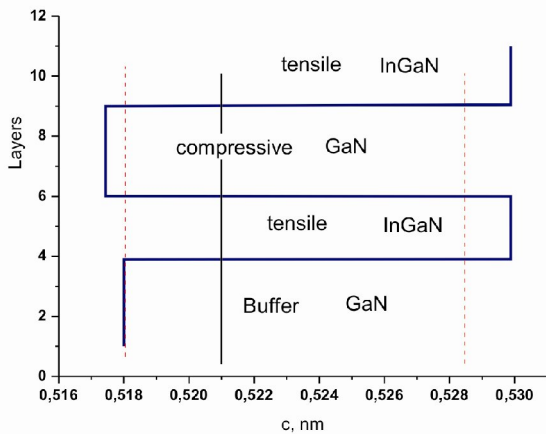
Fig. 2. Schematic figure of the lattice parameter *c* distribution with thickness inside strained SL InGaN/GaN grown on GaN buffer layer. Dashed lines – *c* parameter for unstrained layers, solid lines – average value of *c* parameter for the SL period.

(a)

(b)

Fig. 3. Intensity distribution around reciprocal lattice nodes 0002 (a) and 11-24 (b) in strained SL InGaN/GaN.

This relaxation is fixed on maps of the intensity distribution around reciprocal space nodes, which correspond to asymmetric Bragg's reflections, for which the diffraction vector makes an angle φ with normal to the surface $\vec{n}$. For completely relaxed structure nodes – the centers of reflection of separate layers should lay along the diffraction vector. In the case of partial relaxation, they occupy some intermediate positions. Thus, if the centers of intensity distribution, which correspond to two adjacent layers or to a layer and substrate, are located on the normal $\vec{n}$, relaxation between them does not take place and heterointerface is coherent. Opposite indicates on the presence of relaxation. Our measurement of the intensity distribution around 0002 node of the reciprocal lattice using triple-axis diffractometry shows its periodical character in the direction normal to the sample surface (Fig. 3a). However, the degree of relaxation cannot be determined from the analysis of the symmetric RSM due to the reasons described above. RSM for 11-24 node reflection is presented in Fig. 3b.

Complete relaxation takes place if nodes lay in the direction of the reciprocal lattice vector. In our case, nodes (satellites) of SL lay along the surface normal, but the whole system of satellites is shifted by some distance from GaN buffer layer. The active SL was grown on the buffer SL with a lower indium content. This fact testifies that SL structure was grown on partially relaxed buffer layer.

As A³-nitrides films grown on sapphire relax almost completely at the growing temperature, and stresses observed in them at room temperature are mainly thermal, the previous reasoning can be applied to the buffer layer, so, SL can be characterized by two parameters of relaxation – relaxation of SL as a whole with respect to the buffer layer and relaxation between separate layers of SL.
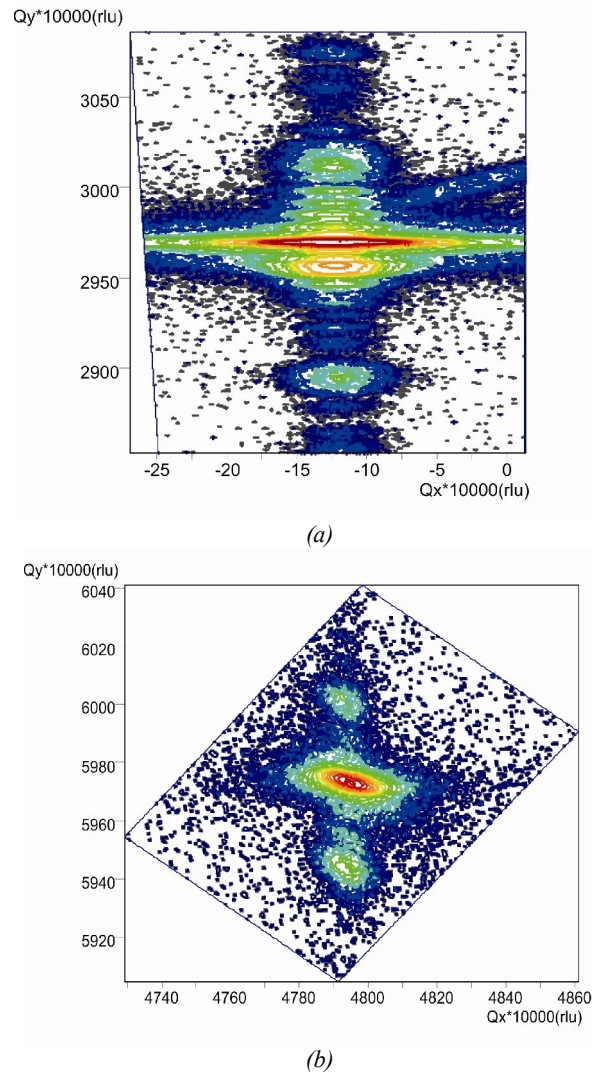
As for complete relaxation of the buffer layer, it is related to the parameters of the lattice of the layer in free condition and is determined with reference to the substrate (the centers of reflection of the layer and substrate lay along **H** direction). Let us note that these reasoning relates to such structures with hexagonal syngony, in all layers of which the ratio of dense packing $c/a = 1.633$ conserves.

Studied $In_xGa_{1-x}N/GaN$ superlattices are characterized by reasonable mismatch of lattice parameters of two layers (more than 1 %) and relatively small thickness of layers and total thickness of SL.

For wurtzite structures (InGaN and GaN layers) that are grown along the hexagonal axis ⟨0001⟩, the lattice parameter *a* determines the interplane distances in the interface plane, parameter *c* – in plane perpendicular to it. Let us designate measured parameters of *i*-th layer in the system as a_i and c_i, and corresponding values for a layer of the same composition in free (unstressed)

condition as a_i^b and c_i^b. The index $i = 0$ corresponds to the buffer layer, and $i = 1, 2$ – to the first and the second sublayers of SL. Elastic deformation of SL layers will be equal to:

$$\varepsilon_i = \frac{a_i - a_i^b}{a_i^b}, \qquad (17)$$

and real parameter $c_i = c_{ib} \cdot (1 - p\, \varepsilon_{ii})$, where $p = 2c_{13}/c_{33}$ is Poisson's ratio. The relaxation of elastic deformations in SL can be characterized by a jump of the lattice parameter $a - \Delta a_i = a_i - a_{i-1}$ on the heterointerface or by the relative level of relaxation

$$r_i = \frac{a_i - a_{i-1}}{a_i^b - a_{i-1}} = \frac{\Delta a_i}{a_i^b - a_{i-1}}. \qquad (18)$$

Values Δa_1 and r_1 correspond to the relaxation on the lower heterointerface (between the buffer layer and the first layer of CP), and Δa_2 and r_2 – to the relaxations on borders between separate layers (Fig. 4). For stressed coherent structure $\Delta a_1 = \Delta a_2 = 0$ and, respectively, $r_i = 0$, and for relaxed layers $r_i = 1$. In our case, as follows from Fig. 4, the growth of lattice parameter a in InGaN layers is observed that points to partial relaxation of these layers ($r_{\text{InGaN}} = 0.015$).

In the case of preservation of the coherence of appropriate layers of SL and its relaxation as a whole with respect to the buffer $\Delta a_2 = 0$, while Δa_1 can be positive or negative depending on the buffer layer composition. In the general case for relaxed non-coherent SL, both jumps of the parameter will not be equal to zero, thus to preserve the periodicity of structure Δa_2 should have the same absolute values at all the borders between SL layers.

As seen from Table and Fig. 2, GaN layers in SL are subjected to stretching ($\varepsilon_{\text{Ga}} > 0$), and layers of solid solution are subjected to compression ($\varepsilon_{\text{InGa}} < 0$), and it takes place for all the investigated structures. The stretching deformation in GaN layers is lower than the compression one in InGaN layers. This difference is mainly caused by the thickness of layers. For all SLs under investigation, the relaxation on the lower heterointerface, *i.e.*, disappearing of stresses between the SL as a whole and the buffer layer, takes place. This is not surprising, taking into account the total thickness of the buffer layer (about 3 μm) and relative mismatch between SL as a whole and buffer layer of GaN (of the order of 0.476 %, proceeding from average SL composition $\langle x \rangle = 0.18$), so the arising stresses far exceed the critical ones.

Epitaxial layers of nitrides grown on the sapphire substrates are characterized by a high density of threading dislocations (up to $10^{10}\,\text{cm}^{-2}$), causing considerable broadening the diffraction rocking curves. Therefore, the classical diffraction pattern with satellites is badly developed on curves of symmetric Bragg's

reflections taken with widely open detector (Fig. 1, curve 1). It is caused by a specific feature of defective structure of nitride films, which is characterized by the high density of threading dislocations, which grow transversely to the surface. This leads to the fact that the diffraction pattern is mainly broadened in a direction parallel to the surface, and its broadening in transversal direction is much lower [19]. The dislocation grids localized on the heterointerface cause stretching the diffraction pattern in the direction transversal to the vector of the reciprocal lattice, regardless of the direction of the latter (see Fig. 1).

The dislocation structure of SL consisting of nitride layers is basically identical to the patterns for single-layered nitride films [20]. As the additional reflection centers (satellites) are distributed along the normal (in the direction of periodic change of the crystal layer composition) they can be fixed on the curves crossing the nodes of the reciprocal lattice in the direction that takes place for ω–2θ-scan in symmetric Bragg's geometry. Satellites are also seen on two-crystal curves obtained in asymmetric grazing-incidence geometry, as the diffracted intensity is integrated in the direction of the greatest broadening (a tangent to Evald's sphere is almost parallel to the surface).

Epitaxial layers and grown monocrystals have different defect structures. The relaxation of mismatch elastic stresses arising due to the difference of lattice parameters of the film and substrate or separate layers among themselves is the basic source for generation of defects in the epitaxial layers [21]. The structure of the layers is characterized by more uniform distribution of defects, high anisotropy of shift fields and appearance of clearly expressed directions — along the surface of the crystal plate (heterointerfaces) and normal to it. Broadening transversely to the vector of diffraction is associated with average turns of blocks and their effective lateral size, the broadening along vector **H** is associated with deformations inside blocks and their sizes in normal direction $\vec{n}$.
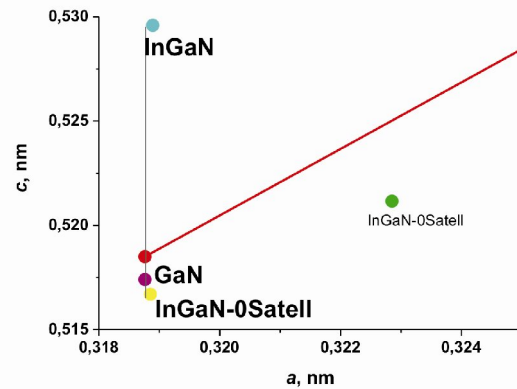

Fig. 4. The lattice parameters of unstrained SL InGaN/GaN. Solid line shows the relaxed value calculated from Vegard's law.

As follows from the analysis of regularities of nodes broadening, dislocation structures of SL layers have a lower dislocation density and more chaotic distribution of dislocations. The stressed condition of SL with respect to the buffer layer testifies the insignificant influence of dislocations in layers of superlattice.

5. Conclusions

The investigation of multilayered structures based on InGaN/GaN compounds that radiate in 460 nm spectral range was carried out using high resolution X-ray diffractometry. Deformation condition of SL and its separate layers, degree of relaxation of the layers of the structure, as well as the period of the SL, thicknesses of the layers and composition of In_xGa_{1-x} solid solution in active area were determined. The method of analysis of experimental rocking curves from multilayered structures with hexagonal symmetry was adapted within the framework of the Parrat-Speriozu model. This made it possible to improve structural parameters and determine the deformation characteristics of the system.

References

1. T. Witaker, Technology and application of light emitting diodes // *LEDs Magazine* **13**, p. 20 (2007).
2. F.A. Ponce and D.P. Bour, Spontaneous polarization and piezoelectric constants of III-V nitrides // *Nature (London)* **386**, p. 351(1997).
3. S. Nakamura and G. Fasol, *The Blue Laser Diode.* Springer, Berlin, 1997.
4. Zhenyang Zhong, O. Ambacher, A. Link, V. Holy, J. Stangl, R.T. Lechner, T. Roch, and G. Bauer, Influence of GaN domain size on the electron mobility of two-dimensional electron gases in AlGaN/GaN heterostructures determined by X-ray reflectivity and diffraction // *Appl. Phys. Lett.* **80** (19), p. 3521 (2002).
5. L. Kirste, K.M. Pavlov, S.T. Mudie, V.I. Punegov and N. Herres, Analysis of the mosaic structure of an ordered (Al, Ga) N layer // *J. Appl. Cryst.* **38**, p. 183-192 (2005).
6. W. Qian, M. Skowronski, M. De Graef, K. Do-verspike, L.B. Rowland, and D.K. Gaskil, Micro-structural characterization of α-GaN films grown on sapphire by organometallic vapor phase epitaxy // *Appl. Phys. Lett.* **66**, p. 1252-1254 (1995).
7. B. Heying, X.H. Wu, S. Keller, Y. Li, D. Kapolnek, B.P. Keller, S.P. DenBaars, and J.S. Speck, Role of threading dislocation structure in the X-ray diffraction peak widths in epitaxial GaN films //*Appl. Phys. Lett.* **68**, p. 643 (1996).
8. T. Metzger, R. Hopler, E. Born, O. Ambacher, M. Stutzmann, R. Stommer, M. Schuster, H. Gobel, S. Christiansen, M. Albrecht, and H.P. Strunk, Defect structure of epitaxial GaN films determined by transmission electron microscopy and triple-axis X-ray diffractometry // *Phil. Mag. A* **77**, p. 1013 (1998).
9. R.N. Kutt, V.V. Ratnikov, G.N. Mosina, M.P. Scheglov, Structural perfection of epitaxial GaN layers in accord to X-ray diffraction data // *Fizika tverdogo tela* **41**, p. 30-36 (1999), in Russian.
10. H.-M. Wang, J.-P. Zhang, C.-Q. Chen, Q. Fareed, J.W. Yang, and M. Asif Khan, AlN/AlGaN superlattices as dislocation filter for low-threading-dislocation thick AlGaN layers on sapphire //*Appl. Phys. Lett.* **81**, p. 604-606 (2002).
11. V.P. Klad'ko, S.V. Chornen'kii, A.V. Naumov, A.V. Komarov, M. Tacano, Yu.N. Sveshnikov, S.A. Vitusevich, and A.E. Belyaev, Interface structural defects and photoluminescence properties of epitaxial GaN and AlGaN/GaN layers grown on sapphire // *Semiconductors* **40**, p. 1060 (2006).
12. M. Yamaguchi, T. Yagi, T. Sota, T. Deguchi, K. Shimada and S. Nakamura, Brillouin scattering study of bulk GaN //*J. Appl. Phys.* **85**, p. 8502 (1999).
13. W. Paszkowicz, X-ray powder diffraction data for indium nitride // *Powder Diffract.* **14**, p. 258 (1999).
14. K.P. O'Donnell, R.W. Martin, and P.G. Middleton, Origin of luminescence from InGaN diodes // *Phys. Rev. Lett.* **82**, p. 237 (1999).
15. V.S. Speriosu, T. Vreeland, Jr., X-ray rocking curves analysis of superlattices // *J. Appl. Phys.* **56**, p. 1591 (1984).
16. V.P. Kladko, A.V. Kuchuk, N.V. Safryuk, A.E. Belyaev, and V.F. Machulin, Influence of dislocation structure on deformation processes in AlGaN/GaN/(0001)Al2O3 heterostructures // *Ukrainian Journal of Physics* **54** (10), p. 1014-1020 (2009).
17. R. Kutt, M. Scheglov, V. Davydov, and A. Usikov, Deformation of layers in superlattice AlGaN/GaN as follows from the X-ray diffraction analysis // *Fizika tverdogo tela* **46** (2), p. 353 (2004).
18. V.P. Kladko, A.V. Kuchuk, N.V. Safryuk, V.F. Machulin, A.E. Belyaev, H. Hardtdegen, and S.A. Vitusevich, Mechanism of strain relaxation by twisted nanocolumns revealed in AlGaN/GaN structures // *Appl. Phys. Lett.* **95**, 031907(3) (2009).
19. V.P. Kladko, A.F. Kolomys, M.V. Slobodian, V.V. Strelchuk, V.G. Raycheva, A.E. Belyaev, S.S. Bukalov, H. Hardtdegen, V.A. Sydoruk, N. Klein, and S.A. Vitusevich, Internal strains and crystal structure of the layers in AlGaN/GaN heterostructures grown on a sapphire substrate // *J. Appl. Phys.* **105,** 063515(9) (2009).
20. V. Ratnikov, R. Kyutt, T. Shubina, T. Pashkova, E. Valcheva, and B. Monemar // *J. Appl. Phys.* **88**, p. 6252-6258 (2000).
21. C. Kisielowski, J. Krüger, S. Ruvimov, T. Suski, J.W. Ager, E. Jones, Z. Liliental-Weber, M. Rubin, E.R. Weber, M.D. Bremser, and R.F. Davis, Strain-related phenomena in GaN thin films // *Phys. Rev. B* **54**, p. 17745 (1996)